Supplementary Materials for

A Self-Reinforcing Hydrogel Disrupting Osteoclast Sealing Zone for Bone Erosion Alleviation

Yilin Wei [1], Bei Kang [1], Baohong Liu [1], Wen Li [1], Yutong Song [1], Mengyao Zhang [1]，Xinyi Liu [1]，Haobo Wang [1]，Zheyi Li [1], Nan Li [1]*

[1] Tianjin Key Laboratory of Drug Delivery & High-Efficiency, School of Pharmaceutical Science and Technology, Faculty of Medicine, Tianjin University, Tianjin 300072, China.

*Corresponding author. Email: linan1985@tju.edu.cn (N. Li).

This PDF file includes:
Fig. S1 to S6
Table S1-S3

CONTENTS

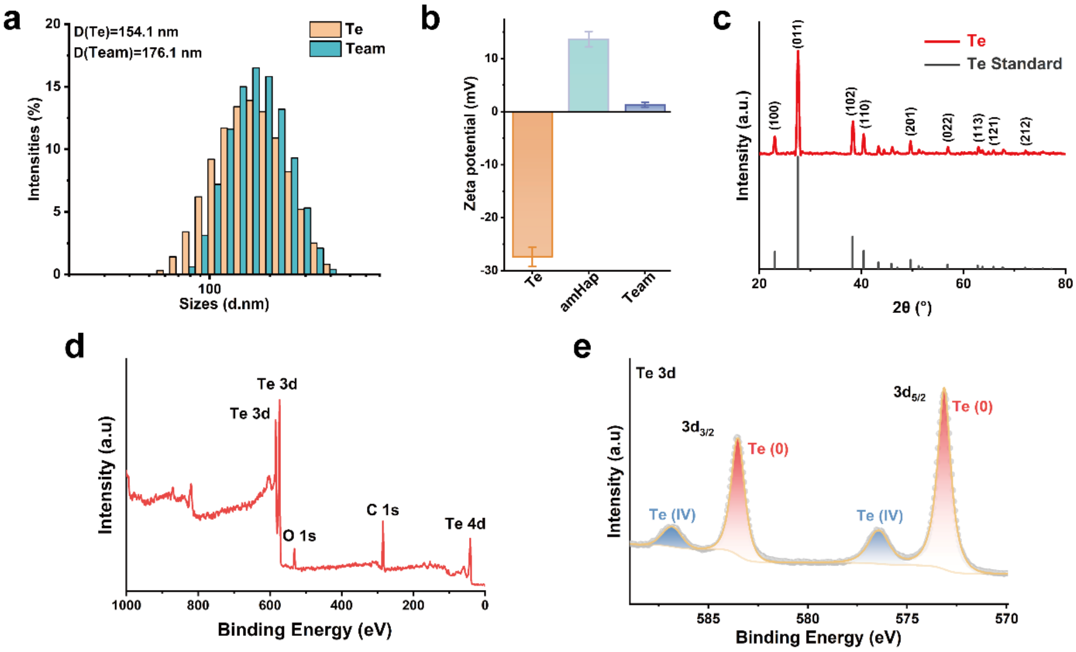

Supplementary Fig. 1 Characterization of Te and Team. a Particle size distribution of Te and Team. **b** Zeta potential of Te and Team. **c** XRD pattern of Te and XRD pattern of Te (JCPDF No.78-2312). **d** Overall XPS pattern of Te. **e** High-resolution XPS pattern of Te 3d in Te.

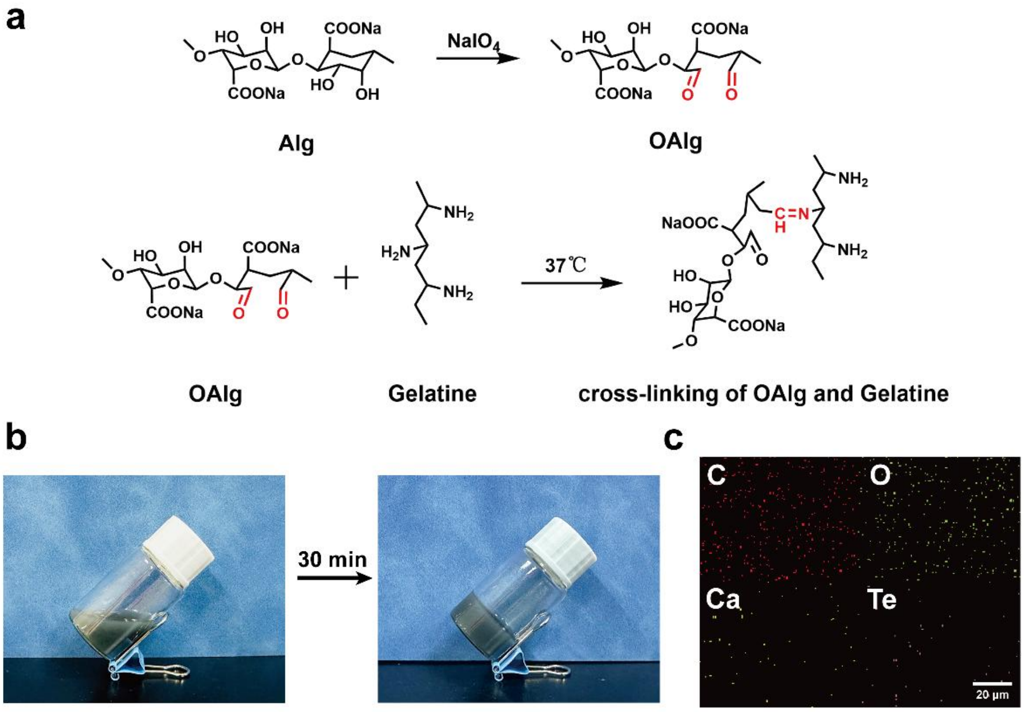

Supplementary Fig. 2 Preparation and characterization of Team Gel. a Synthetic procedure of Team Gel. **b** Images of Team Gel were captured before and after cross-linking. **c** Elemental mapping of C, O, Ca, and Te in the Team Gel.

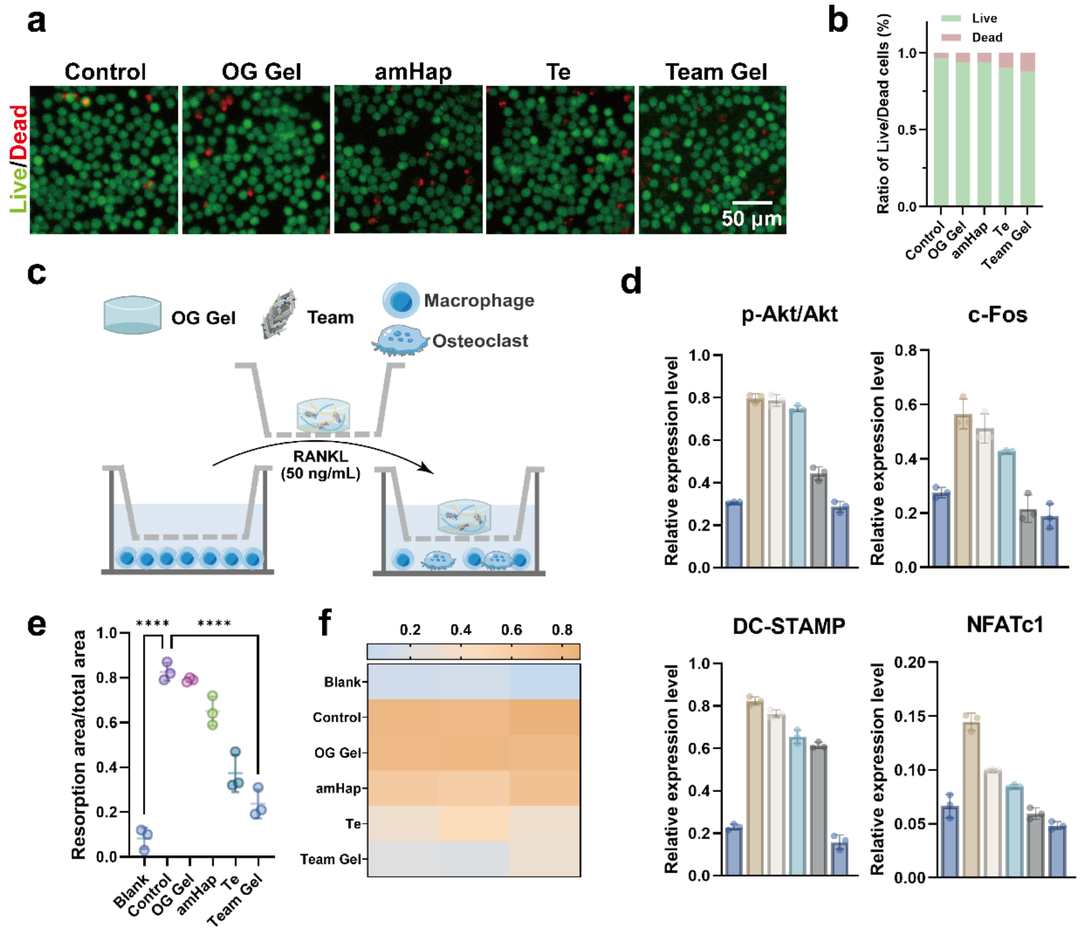

Supplementary Fig. 3 Cellular biocompatibility and effects of Team Gel. a Fluorescent images and quantitative evaluation of RAW264.7 co-stained by Calcein AM/PI. **b** Green (Calcein AM), live cells; red (PI), dead cells. **c** Schematic of osteoclast precursors in noncontact coculture with hydrogels in a 12-well transwell plate. **d** Western blot analysis of protein levels of Akt, p-Akt, c-Fos, NFATc1 and DC-STAMP in osteoclasts. **e** Quantitative analysis of bone resorption area. **f** Heatmap of quantitative analysis of bone resorption area. Data were presented as the mean ± SD (n = 3 independent experiments). $^*P < 0.05$, $^{**}P < 0.01$, $^{***}P < 0.001$, and $^{****}P < 0.0001$. Statistical comparisons were performed using one-way ANOVA with Tukey's test. Source data are provided as a Source Data file.

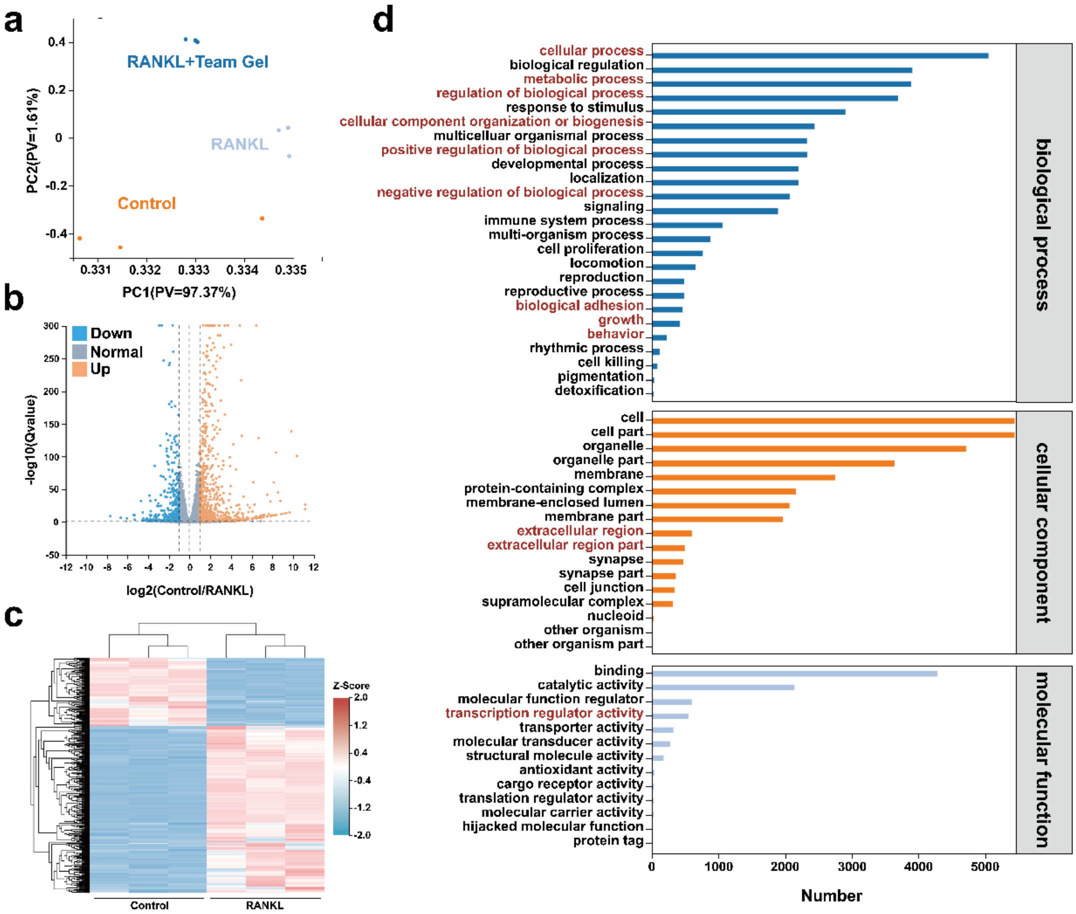

Supplementary Fig. 4 Team Gel-induced transcriptional reprogramming achieved inhibition of osteoclast generation and function. a PCA of genes in RAW 264.7 (control group) or RANKL-activated RAW 264.7 before treatment (RANKL group) or after treatment with Team Gel (RANKL+ Team Gel group). **b** Volcano plots for the Control versus the RANKL groups comparisons. Upregulated genes are marked orange, and downregulated genes are marked blue. **c** Heatmap showing the hierarchical clustering of the differentially expressed genes in Control and RANKL groups. **d** GO enrichment bar plots of Control and RANKL groups.

Supplementary Fig. 5 ACLT model in male rat knee joints for OA. Images of the male rat OA model with standardized anterior cruciate ligament transection (ACLT) in the left knee joints.

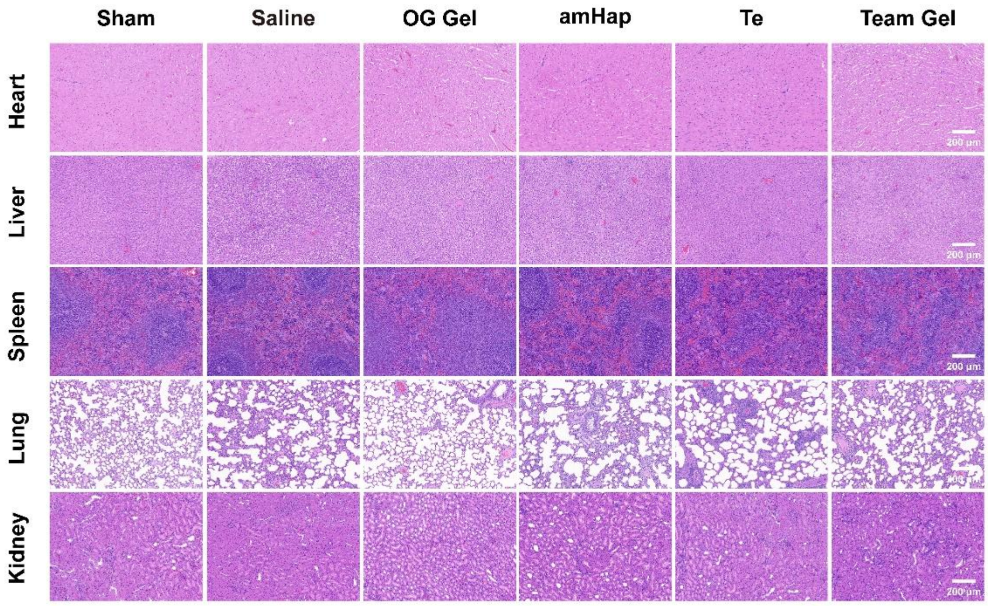

Supplementary Fig. 6 Histological analysis of major organs. Representative histological images for major organs, including heart, liver, spleen, lung, and kidney with H&E staining.

Table S1. The sequence of primers used in RT-qPCR.

Gene	Forward primer (5’-3’)	Reverse primer (5’-3’)
GAPDH	GCAAGTTCAACGGCACAG	CCAGTTGGTAACAATGCCATGT
C-Fos	TATTCCGTTCCCTTCGGATT	GGTGAAGACCGTGTCAGGAG
NFATc1	TCTGGACCTGGGTGATGGGG	GATACGAGGCCTGTGGCACC
DC-STAMP	AAAACCCTTGGGCTGTTCTT	AATCATGGACGACTCCTTGG

Table S2. OARSI Histopathology Scoring System Template for Rat Knee OA

Parameter	Score Range	Scoring Criteria
Grade (Depth of lesion)	**0–6**	0 = Normal cartilage surface 1 = Surface irregularities (minimal fibrillation) 2 = Pannus and superficial fissures 3 = Vertical clefts extending into mid-zone 4 = Vertical clefts into deep zone 5 = Erosion to calcified cartilage 6 = Denudation of cartilage, deformation of subchondral bone
Stage (Extent of lesion)	**0–4**	0 = No involvement 1 = <10% of the surface 2 = 10–25% of the surface 3 = 25–50% of the surface 4 = >50% of the surface
Score (Grade × Stage)	**0–24**	Multiply Grade and Stage to generate total score per site (e.g., medial tibial plateau)

Table S3. List of abbreviations.

Abbreviation	Definition
OA	Osteoarthritis
MMP	Matrix metallopeptidase
Te	Tellurium
NP	Nanoparticle
am	Amino
Hap	Hydroxyapatite
Ca^{2+}	Calcium ion
SB	Subchondral bone
RANKL	Receptor activator of NF-κB ligand
Se	Selenium
F-actin	Filamentous actin
PO_4^{3-}	Phosphate ion
H_2SeO_3	Selenous acid
TeO_2	Tellurium dioxide
$Ca(NO_3)_2$	Calcium nitrate
$(NH_4)_2HPO_4$	Ammonium phosphate dibasic
SDS	Sodium dodecyl sulfate
TEM	Transmission electron microscopy
DLS	Dynamic light scattering
SAED	Selected area electron diffraction
XRD	X-ray diffraction
TeO_3^{2-}	Tellurite ion
H_2O_2	Hydrogen peroxide
APTES	γ-Aminopropyltriethoxysilane
FTIR	Fourier-transform infrared spectroscopy
FITC	Fluorescein Isothiocyanate

OGGel	Oxidized alginate and gelatin hydrogel
OGTH	OGGel-TH hydrogel
OAlg	Oxidized alginate
SEM	Scanning electron microscopy
G′	Stable storage modulus
G″	Loss modulus
CCK8	Cell Counting Kit-8
OC	Osteoclast
CTSK	Cathepsin K
ELISA	Enzyme linked immunosorbent assay
TRAP	Tartrate - Resistant Acid Phosphatase
ACLT	Anterior cruciate ligament transection
OARSI	Osteoarthritis Research Society International
DEGs	Differentially expressed genes
GO	Gene ontology
KEGG	Kyoto Encyclopedia of Genes and Genomes
Sham	Sham-operated
Micro-CT	Micro–computed tomography
H&E	Hematoxylin-eosin
BMD	Bone mineral density
BV	Bone volume
TV	Tissue volume
Tb. N	Trabecular number
Tb. Th	Trabecular thickness
Tb. Sp	Trabecular separation/spacing
SD	Standard deviation
PBS	Phosphate buffered saline
RT	Reverse transcription
PCR	Polymerase chain reaction

DMEM	Dulbecco's modified eagle medium
DAPI	4′,6-diamidino-2-phenylindole
H&E	Hematoxylin and eosin
IHC	Immunohistochemical
ECM	Extracellular matrix
COL2A1	Collagen Type II Alpha 1 Chain
ANOVA	One-way analysis of variance